PHYSICO-MECHANICAL, MORPHOLOGICAL AND THERMAL ANALYSIS OF BIOPLASTIC FILMS FABRICATED FROM SAGO PITH WASTE CELLULOSE FIBRES

NURUL FARHANA ZABIDI*, JOSEPHINE LAI CHANG HUI

Department of Chemical Engineering and Energy Sustainability, Faculty of Engineering,
Universiti Malaysia Sarawak, 93400, Kota Samarahan, Sarawak, Malaysia
*Corresponding Author: nurulfarhanazabidi@gmail.com

Abstract

In light of the growing demand for sustainable alternatives to traditional plastics and the world's mounting environmental problems, this research explores the field of bioplastics with an emphasis on sago pith waste (SPW). The growing demand for biodegradable materials makes it essential to utilise resources such as SPW, which are plentiful in biomass, especially from the sago industry in Sarawak. The extraction of sago starch has led to significant environmental issues due to inadequate waste management practices. Therefore, while focusing on utilizing SPW, this research aims to fabricate a bioplastic film from SPW and investigate the optimal mass of cellulose fibres (CF) extracted from SPW solubilized in 20 mL of trifluoroacetic acid (TFA) to form a bioplastic film with good properties. First, to extract CF, the SPW underwent alkaline treatment and bleaching treatment. Then, CF was solubilized in TFA, with varying in mass from 0.10 g to 0.70 g. After the CF was fully dissolved, the process was then followed by solvent casting. The resulting bioplastic films produced were transparent with slight brown coloration. The SEM data revealed that bubble-shape protrusions on the bioplastic films appeared to shrink as the mass of CF decrease and a slight decrease in the number of visible pores were noted. Due to the improved morphological properties of the film, the tensile strength of BF-0.70 was enhanced by 90% as compared to BF-0.10. BF-0.70 also exhibited the best thermal stability as the main component of the bioplastic film started to degrade at 193°C and had the most amount of char residue. Out of all the other films, BF-0.70 also possessed the least water absorption ability, with a value of 86%, which was a good decrease from the 198% water absorption by BF-0.10. Thus, it was possible to determine the ideal CF mass. As evidenced by the features of BF-0.70, the results had proven that 0.70 g is the optimal mass of CF that can be solubilised in TFA to form a bioplastic film with good properties.

Keywords: Alkaline treatment, Bioplastic films, FTIR, Sago pith waste, SEM, Solvent casting, Sustainable materials, Tensile strength, TFA, TGA, Water absorption.

1. Introduction

Today, fossil fuels, namely petroleum, are the main source of plastic. Approximately three-quarters of each barrel of oil is used to produce gasoline, diesel, and jet fuel; the remaining one-fourth is used to produce other goods, such as plastic [1]. In 2022, more than 390 million tonnes of fossil fuel-based plastics were manufactured, and plastic pollution has since grown to be a serious threat to both human and ecological health [2]. The continual consumption of fossil fuels for energy and manufacturing processes have led to the fast depletion of these non-renewable resources.

Therefore, it is significant to note that the future challenge of fossil fuel depletion has prompted research into the development of sustainable materials and alternatives, such as bioplastics [3]. The production of bioplastics is gaining popularity as a potential replacement for polymers derived from fossil fuels. Biopolymer's raw materials are made from biomass; therefore, they are more renewable than other materials. Some bioplastics are also very biodegradable, which makes them a more environmentally sustainable material [4].

These bioplastics can not only help decrease the need for fossil fuels, but they can also aid in reducing problems regarding waste disposal, which has become a global concern due to human activity's impact on the environment. The implementation of new laws and policies, as well as continued attention, are required for global efforts aimed at creating and improving ways to reduce soil, water, and air pollution [5].

In light of this, there is a growing recognition of the importance of implementing sustainable practises for the extraction of sago starch from sago (*Metroxylon sagu*), that has huge potential to become a versatile crop and help strengthen the food security program, thus becoming the next viable food commodity in Sarawak. This is because it has impressive high starch yield when compared to other sources such as corn, rice, and wheat [6]. It was found that over 400 kg of dry starch can be obtained in a sago palm tree and the yield can go as much as 25 metric tons per hectare [7]. Thus, initiatives have been taken by the Sarawak government to encourage sago plantation to a bigger scale which is estate plantation, an upgrade from small-scale farming that has long been done by the natives [8].

The rapid production of sago starch leads to an increase of generated waste during the extraction process. Sago starch is obtained from the rasped pith of the sago palm, leaving fibrous residues called sago *hampas* or sago pith waste (SPW) that contains an abundant amount of sago starch trapped inside the lignocellulosic fibre matrix which composed of lignin, cellulose, and hemicellulose [9]. The huge amount of sago waste generated by the sago starch extraction process has caused many environmental challenges due to improper waste management practices.

Most owners of sago mills do not recover the sago biomass and discharge the SPW to the nearby river with sago effluents without any treatment or the waste will be incinerated, which can cause serious environmental issues such as water pollution and air pollution [10]. For per ton of dried starch extracted by using the current available process, there are around 3 tons of sago pith waste and 0.5 tons of sago bark waste produced. Meanwhile, after processing between 8 and 12 logs on an industrial scale, the daily sago pith waste production can vary from 3 to 5 tonnes

[11]. The lack of efficient strategies for handling and transforming sago waste into higher value-added materials can lead to environmental pollution and resource wastage [12].

However, the utilization of SPW as a raw material for bioplastic production holds great promise in addressing both waste management and sustainable resource utilization. Nevertheless, raw SPW could not be used to produce higher value-added materials because of the composition of the waste. From previous research, starch had been extracted from SPW through assistance of ultrasound to form a bioplastic [13] and CF were extracted from treating SPW through alkaline treatment and bleaching treatment. Yacob et al. had treated SPW by using alkaline and bleaching treatment to extract CF to act as a reinforcing agent, specifically to improve the properties of starch films produced in the study [14]. Meanwhile, Jampi et al. also used similar techniques to extract CF from SPW, before preparing it into hydrogel [15]. Therefore, the treatments to extract CF were applied in this study, as past research had used cellulose-based raw materials to form a bioplastic film by solubilizing in trifluoroacetic acid (TFA) and solvent casting [16].

In addition, a method discovered by Bayer et al. uses TFA as a solvent to solubilize cellulose and similar compounds as well as several agricultural plant wastes to form bioplastic films [17]. TFA aids in the formation of a homogenous solution that can be cast into a bioplastic film. Due to its ability to swell cellulose effectively and its ability to be recycled because of its low boiling point, trifluoroacetic acid (TFA) is of interest since it offers an effective method to reduce cellulosic crystallinity and break up hydrogen bonds within the crystalline region [18]. While TFA has shown promise in creating bioplastics from various sources, such as rice hulls, green herbs, cocoa pod husks, and seaweed [19], a substantial research gap persists. Currently, there is no research that uses CF extracted from SPW to produce bioplastic films by using TFA. Furthermore, there is a lack of investigation into identifying the suitable mass of cellulose fibres (CF) from SPW in a fixed volume of TFA.

Consequently, the influence of CF mass on critical properties of resulting bioplastic films—including morphology, mechanical strength, thermal characteristics, and water absorption—remains unexplored. Addressing this gap is crucial for optimizing the production process and enhancing the overall performance of bioplastic films. Therefore, the research focuses on addressing this research gap by investigating the effects of the different masses of CF in a fixed volume of TFA on the properties of the resulting bioplastic films. In addition, the FTIR, morphological, mechanical, and thermal properties as well as water absorption of bioplastic films produced were also analysed.

To achieve these objectives, the methodology involved systematically varying the masses of CF within a fixed volume of TFA. The subsequent bioplastic films were subjected to several analyses, encompassing evaluations of FTIR spectra, morphological characteristics, mechanical strength, thermal behaviour, and water absorption properties.

2. Methodology

The SPW was collected from Kampung Skibang, Bau. Fresh SPW were washed to remove dirt and impurities. Then, the cleaned SPW was soaked in a 40 °C distilled water to get rid of excess starch [14] and was dried in an oven. After drying, SPW

was grounded into find powder using analytical grinder at the speed of 3 for 5 minutes and sieved through a screen. The fine powder expanded the amount of surface area that the alkali and bleaching solutions could access during CF extraction [20].

2.1. Extraction of cellulose

The extraction of cellulose from SPW was carried out based on methods used in previous works [14, 15]. The SPW was treated with 4% w/v sodium hydroxide (NaOH) and bleached with sodium chlorite (NaClO$_2$) and acetic acid solution.

2.1.1. Alkaline (NaOH) treatment

10 g of SPW was weighed and dried in an oven overnight to remove excess moisture. Then, the 500 mL of 4% NaOH was poured into a beaker and placed on top of a hot plate with the temperature maintained at 70 °C. Any excessive concentrations or temperatures combined as well as prolonged processing times can lead to structural damage to cellulose, increased energy requirements, and increased operating expenses [21].

Then, the SPW was immersed into the beaker and the solution was stirred by using a magnetic stirrer of speed 1500 rpm. This process was done for one hour. Then the solution was filtered to obtain the remaining solute by using a Buchner flask, Buchner funnel, filter paper and vacuum pump. This process was repeated three times to ensure effectiveness. This method was carried out based on the previous work done by Jampi et al. [15].

During this treatment, the NaOH solution was used to help separate the cellulose fibres from the lignin and hemicellulose components of the SPW [22]. Alkaline treatment would modify the fibre network structure by breaking down the OH bonding present in the SPW. This was accomplished by converting the hydroxyl groups of the various materials present in the fibres into alkoxide ions through ionization as shown in Eq. (1).

$$Fibre - OH + NaOH \rightarrow Fibre - O^-Na^+ + H_2O \tag{1}$$
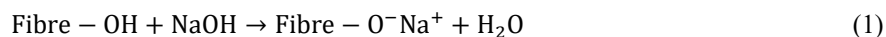
2.1.2. Bleaching (NaClO2) treatment

The remaining solute underwent bleaching with a solution containing 160 mL of distilled water, 1 mL of glacial acetic acid (CH$_3$COOH) and 1.5 g of sodium chlorite (NaClO$_2$) [23]. This process was done by using a screw-top Erlenmeyer flask that was placed inside a water bath that was maintained at 70 °C for 3 hours [23]. The concentration, temperature and duration of the bleaching treatment were optimized to avoid excessive bleaching conditions that would cause severe oxidation of celluloses and significantly reduced their dimension [24].

This process was repeated three times to ensure effectiveness. The method was also carried out based on previous work done by Pushpamalar et al. [23]. When the bleaching process was done, the solution was filtered with a Buchner flask, Buchner funnel, filter paper and a vacuum pump. During bleaching, the reaction between lignin and sodium chlorite results in the formation of lignin chloride, which can be removed by continuous washing with distilled water since it dissolves in the medium [25].

Therefore, after filtering, CF was obtained and cleaned thoroughly with distilled water until the pH of solvent obtained in Buchner flask was neutral [14]. The CF

was then dried in the oven at 40 °C overnight. Table 1 below shows the product yield of the treatment of SPW calculated by using Eq. (2).

$$\text{Product yield} = \frac{\text{Mass of product (g)}}{\text{Mass of SPW}} \times 100 \qquad (2)$$

Table 1. Product yield of alkaline and bleaching treatment of SPW.

	Mass of product	Product yield (%)
10.00 g of SPW	0.34	3.40
	0.43	4.30
	0.42	4.20
	0.30	3.00
	0.40	4.00
Mean	0.38	3.78

2.2. Solubilisation of CF in TFA

To avoid any moisture, the CF was dried again by placing it in a 40 °C oven overnight. The next day, 0.10 g of CF was weighed and placed in a reagent bottle containing 20 mL of TFA. 20 mL of TFA was used as past research also used 20 mL of TFA to solubilize their raw materials and formed bioplastic films [26]. The reagent bottle was placed in a water bath that was maintained at 50 °C on a hot plate. The solubilisation was done at 50 °C temperature so that the process would be accelerated [27]. All the mixture was then stirred with a magnetic stirrer for three days at 600 rpm in order to ensure effective solubilisation of CF. The mixture was then centrifuged to separate the impurities and undissolved component of CF such as silica bodies [26].

These methods were carried out based on previous work done by Bayer et al. [26], Bilo et al. [16] as well as two research carried out by Guzman-Puyol et al. [28, 29]. The procedure was repeated with different weight of CF, which are 0.30 g, 0.50 g, and 0.70 g. These masses were chosen based on the recommendation by Bayer et al., which states that the starting material should typically start with 0.5% by weight in TFA solution, which is around 0.1 g in 20 ml TFA.

They also stated that the preferred amount of starting material is from 1% to 2% by weight, which is around 0.3 g to 0.6 g of starting material in 20 ml of TFA [16, 26-29].This research was not able to produce a bioplastic with 0.9 g of CF probably due to oversaturation.

The solution was cast in a Petri dish to obtain free-standing bioplastic films and placed in a fume hood to let the solvent evaporate overnight. The films were labelled as BF-0.10, BF-0.30, BF-0.50 and BF-0.70 in which BF stands for bioplastic film and the numbers refer to the amount of CF solubilized in 20 mL of TFA as shown in Table 2.

Table 2. Bioplastic films label.

Mass of CF in 20 mL of TFA	Label
0.10 g	BF-0.10
0.30 g	BF-0.30
0.50 g	BF-0.50
0.70 g	BF-0.70

2.3. Characterization of bioplastic films

The bioplastic films had undergone Fourier transform infrared spectroscopy (FTIR), scanning electron microscopy (SEM), tensile test, thermogravimetric analysis (TGA) and water absorption.

2.3.1. Fourier transform infrared spectroscopy (FTIR) analysis

Fourier transform infrared attenuated total reflectance spectroscopy (FTIR-ATR) was carried out. The spectra were analysed on Shimadzu IRAffinity-1 in the 4000-600 cm^{-1} regions with a resolution of 1 cm^{-1} [26]. Wavelength 4000 to 600 cm^{-1} was chosen because there is no significant wavelength to be detected from 0 to 600 cm^{-1}.

In addition, this study uses FTIR analysis to quickly, and effectively identify functional groups and identify any potential chemical alterations in the SPW after treatment and the bioplastic film samples formed.

2.3.2. Morphological properties analysis

Scanning electron microscope (SEM) images of the SPW, CF, and all the bioplastic films produced were taken by using SEM (Hitachi TM4000Plus Tabletop Microscope, Tokyo, Japan). The images were taken from the surface of the samples and were collected at magnification of ×1000 with energy of the beam at 15kV.

2.3.3. Mechanical properties analysis

For tensile strength and Young's modulus evaluation, a tensile test was carried out by using universal testing instruments (Shimadzu Autograph AGS-S50kNX, Japan). The crosshead speed was 0.5 mm/min, with sample's testing length and width to be 40 mm and 5 mm, respectively. This method followed the standard test method for tensile properties of thin plastic sheeting (ASTM D882).

2.3.4. Thermal properties analysis

Thermogravimetric analysis was carried out to establish thermal stability of bioplastic by using TG Analyzer Spectrum 500 and analysed by the Universal Analysis 2000 between 30 °C and 600 °C with a heating rate of 10 °C/min. The standard test method is ASTM E1131-20. TGA curves were obtained from the analysis.

2.3.5. Water absorption test

This test was conducted using ASTM D570, the standard industry method for calculating plastics' water absorption. The bioplastic film sample with a known weight that had already been dried for 24 hours at 65 °C was submerged in water for 24 hours in a 100 mL beaker of distilled water.

After the experimental time, the sample was removed from the water, patted dry with a lint free cloth, and then weighed. The percentage of water absorbed was calculated by using Eq. (3) where w_0 is the initial weight and w_1 is the final weight of the sample. Each sample was tested 3 times, and the mean and standard deviation of the calculated water absorption percentage were calculated.

$$\text{Water absorbed} = \frac{w_1 - w_0}{w_0} \times 100 \qquad (3)$$

3. Results and Discussion

3.1. Cellulose extraction from SPW

Observationally, bleached cellulose fibres extracted from SPW changed colour to white, clearly showing that most of the original non-cellulosic components had been removed [30] as seen in Fig. 1.
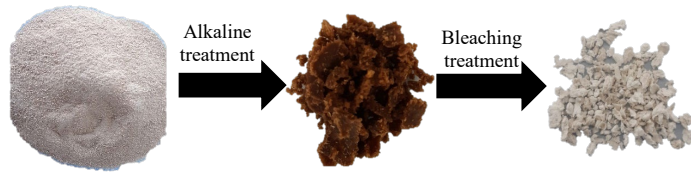

Fig. 1. Extraction of cellulose from SPW.

It was also observed that a minor portion of the cellulose was brownish, which was due to the residual non-cellulosic component that were undissolved during both treatments. This finding aligned with existing research which indicated that as the undissolved non-cellulosic content in the cellulose fibre increased, there was a corresponding decrease in their brightness or whiteness level [21]. Similar studies had proven that the treatments did not completely remove the non-cellulosic components of the raw materials. After the alkaline and bleaching of sago frond to extract cellulose, the non-cellulosic component of sago frond was not completely removed as the whiteness of cellulose sago frond was 79.13% and had relatively low content of lignin and hemicellulose [21]. Another study also had extracted cellulose from pineapple leaf fibre through alkali and bleaching treatment [30]. They also found that the residual lignin in the cellulose fibres was around 0.4% to 2.8%. Therefore, this past research confirmed that the treatments did not completely remove the non-cellulosic component of the SPW, and these components were still present in the cellulose fibres obtained.

3.2. Production of bioplastic films

Table 3 showed the observation recorded from Day 1 to Day 3 of the solubilisation of 0.10 g, 0.30 g, 0.50 g, and 0.70 g of CF in 20 mL of TFA. On the first day, the CF was immersed in 20 mL of TFA. Upon observation, CF started to swell immediately after immersing in TFA. After several hours depending on the amount of CF, it was observed that the cellulose solution was homogenous, indicating the solubilisation of CF. To standardise the bioplastic films forming process, the solubilisation process of all CF in 20 mL of TFA was done 3 days to ensure effective solubilisation of CF [27]. After 3 days, the bioplastic films were cast in Petri dishes. The formulation has successfully produced free-standing bioplastic films as shown in Fig. 2. Based on the Tables, it was observed that the lower the mass of CF immersed in the TFA, the faster the solubilisation process. The smaller amount of cellulose meant that there was smaller amount of cellulose polymer chains to be disintegrated [31].
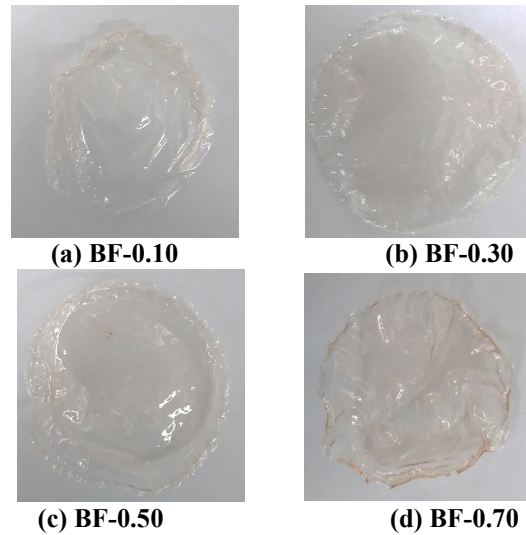
(a) BF-0.10   **(b) BF-0.30**

(c) BF-0.50   **(d) BF-0.70**

Fig. 2. Bioplastic films after CF digestion in TFA.

Table 3. Observation recorded from
day 1 to day 3 of the solubilisation of CF.

Mass of CF (g)	Observation recorded from Day 1 to Day 3 of the solubilisation of CF	Time taken to solubilise
0.10		6 hours
0.30		12 hours
0.50		26 hours
0.70		32 hours

After the solvent was completely evaporated, the bioplastic films produced were transparent as shown in Fig. 2 but exhibited a distinct brown coloration, with BF-0.70 being the most intense. This was due to the increasing amount of brownish portion of the cellulose, which was the residual non-cellulosic component present in the CF, as

the amount of CF dissolved in 20 mL of TFA was increased. This was proven again by similar research which stated that the bioplastic films produced exhibited brown coloration due to the presence of a high number of organic compounds in the matrix [16]. In context, instead of cellulose, TFA can partially break down lignin and hemicellulose as well as other non-cellulosic polysaccharides [17, 26].

3.3. Fourier transform infrared spectroscopy (FTIR) analysis of bioplastic films

Figure 3 shows the FTIR spectra for BF-0.10, BF-0.30, BF-0.50, BF-0.70, and CF. By observing the spectra, it was apparent that all four bioplastic film spectra exhibit negligible differences in their respective spectral profiles as compared to the CF spectrum.
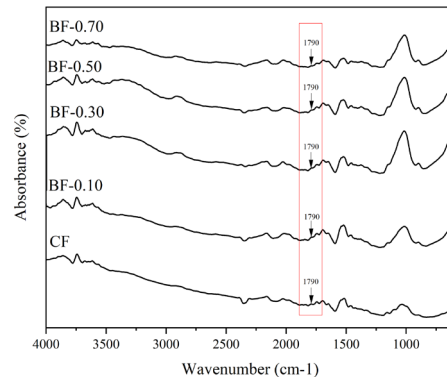

Fig. 3. FTIR spectra of CF, BF-0.10, BF-0.30, BF-0.50, and BF-0.70.

The peaks at 1015 cm^{-1} to 1037 cm^{-1} corresponds to C-O stretching that is commonly found in cellulose, hemicellulose, and lignin [15]. It is observed that the peak of 1037 cm^{-1} in CF shifted to 1015 cm^{-1} in the bioplastic films spectra, probably indicating a decrease in the crystallinity. The TFA disrupts the intermolecular hydrogen bonds within the cellulose structure. This disruption causes the cellulose molecules to rearrange, adopting a less ordered state.

The appearance of a peak at 1520 cm^{-1} in all concentrations of bioplastic films was attributed to the aromatic skeletal vibration (C-C stretching), indicating the presence of lignin in the CF [32] that was mentioned in Section 3.1 and was solubilised in TFA to form a bioplastic film. The lignin had also contributed to the thermal stability of the bioplastic films, which will be discussed in Section 3.6.

Meanwhile, the peak 1645 cm^{-1} corresponded to O-H bending that indicated the presence of absorbed water [33]. According to a study of cellulose bonding with TFA done by Monika [34], a peak around 1790 cm^{-1} appeared in the cellulose-TFA sample, which was attributed to the carbonyl group (C=O) of the cellulose trifluoroacetate. For this study, there were no changes in 1790 cm^{-1} peak which indicated that there are no trifluoroacetylated residue in the films.

The TFA was evaporated during the casting process in order to form a free-standing bioplastic film. The small broad peak observed at around 2890 cm^{-1} was attributed to the stretching vibration of C-H, which are present in all hydrocarbons present in the samples [35]. The presence of a wide broad peak in the 3500 cm^{-1} to 3000 cm^{-1} regions

for all spectra of bioplastic films was due to the presence of hydroxyl (O-H) functional group that can be found in cellulose and hemicellulose [36].

Based on the findings, the FTIR analysis of bioplastic films showed peaks similar to the CF spectrum that corresponded to the presence of functional groups. It was apparent that there were no notable differences in peak patterns of the bioplastic films formed when compared with the CF that was solubilized in TFA. The functional groups indicated the presence of cellulose and non-cellulosic components, as well as absorbed water.

3.4. Morphological properties analysis of bioplastic film

Figure 4 below shows the SEM images of BF-0.10, BF-0.30, BF-0.50, and BF-0.70 at 1000×. Furthermore, it was observed that the texture of the surface had bubble-shape protrusions on the surface. As the mass of CF solubilized in TFA got higher, the bubble-shape texture appeared to decrease in size, and slight reduction in the number of visible pores were observed. This was most probably due to the more adequate distribution of the CF within the matrix as the mass increased [37], especially for BF-0.70 as the bubble-shape protrusions was the smallest among all the bioplastic films and had a smooth surface.

The more adequate distribution leads to a more homogeneous structure, reducing the size of surface irregularities and enhancing the overall smoothness of the film. They also serve as a starting point for a more thorough investigation of how these morphological variations had impacted the mechanical and other performance characteristics of the bioplastic films.

The relationship between the surface characteristics that were observed, and the mechanical properties of the bioplastic films is noteworthy. The decrease in bubble-shape protrusions and the appearance of the smoother surface of BF-0.70 had suggested a uniform distribution of CF, which was likely to affect the tensile strength and other properties. These SEM data had offered a visual representation of the structural changes caused by the different masses of CF, as will be discussed in more detail in later sections.
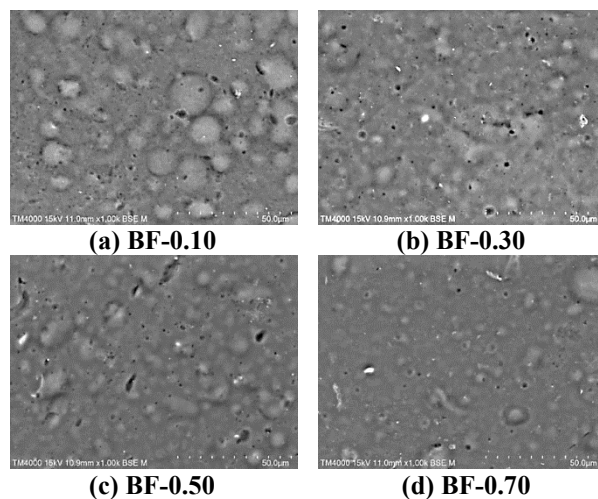

(a) BF-0.10   (b) BF-0.30

(c) BF-0.50   (d) BF-0.70

Fig. 4. SEM images for bioplastic films at 1000×.

In addition, the SEM data of BF-0.70 at ×500 was compared with a bioplastic film made from sago starch filled with cellulose microfibres (SSCMF) from water hyacinth [38]. The SEM images showed similar surface characteristics, including agglomerations of cellulose microfibers and pores. Meanwhile, at 500×, the BF-0.70 produced in this study was also smooth, pores, and agglomerations that was due to undissolved CF during solubilization in TFA.

3.5. Mechanical properties analysis of bioplastic films

Tensile tests were conducted on all bioplastic films, BF-0.10, BF-0.30, BF-0.50, and BF-0.70. The tensile strength and Young's modulus of the bioplastic films can be observed in Tables 4 and 5, and Fig. 5. It was implied that BF-0.70 had the highest tensile strength and Young's modulus, followed by BF-0.50 and then BF-0.30. BF-0.10 had the lowest tensile strength and Young's modulus. This showed that of the four samples, BF-0.70 was the strongest and most rigid, whereas BF-0.10 was the weakest and least rigid. BF-0.70 had the highest tensile strength and Young's modulus value.

The higher the amount of CF immersed in TFA, the higher the amount of cellulose bonds within and between cellulose chains in the formed bioplastic film, which are proven to be crucial for improved mechanical properties of the bioplastic films [39]. The surface texture of the bioplastic films as shown in the SEM images also affected the tensile strength of the bioplastic films. The texture of the bubble-shape protrusions on the surface caused mechanical measurement samples to be non-uniform in term of cellulose distribution in the bioplastic films matrix, which affected the results of the mechanical analysis [40].

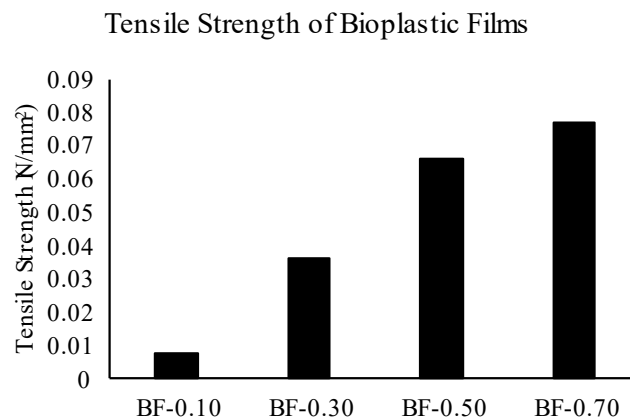Fig. 5. Tensile strength of bioplastic films.

Table 4. Tensile strength results.

	Sample 1 (%)	Sample 2 (%)	Sample 3 (%)	Mean (%)	Standard deviation (%)
BF-0.10	0.005	0.01	0.008	0.008	0.01
BF-0.30	0.029	0.045	0.033	0.036	0.01
BF-0.50	0.067	0.06	0.07	0.066	0.01
BF-0.70	0.078	0.075	0.089	0.081	0.01

Table 5. Young's modulus results.

	Sample 1 (%)	Sample 2 (%)	Sample 3 (%)	Mean (%)	Standard deviation, (%)
BF-0.10	0.287	0.273	0.300	0.287	0.010
BF-0.30	1.01	1.049	1.061	1.040	0.030
BF-0.50	1.709	2.012	1.827	1.849	0.150
BF-0.70	2.532	2.943	2.685	2.720	0.200

The tensile strength and Young's modulus of the bioplastic film would be affected by the pores, provided they showed a weakness in the film's rigidity. The empty spaces or gaps within the material's structure which have been known as pores, can have an impact on a film's ability to endure stretching or deformation without breaking. This had an impact on the bioplastic film's overall rigidity, or its ability to maintain its shape and resist deformation. As a result, the tensile strength and Young's modulus are decreased [41].

When compared to the SSCMF bioplastic film, it was apparent that SSCMF bioplastic films had better mechanical properties with 7.0 N/mm^2 of tensile strength as compared to BF-0.70 that had only 0.081 N/mm^2 of tensile strength. One of the possible reasons was SSCMF [38] used starch as the matrix and the cellulose microfibres as a filler that can enhance the mechanical properties of the bioplastic film whereas the film in this research did not incorporate any fillers in the matrix. One bioplastic film had cellulose fibres as fillers and starch as a matrix; another had no reinforcement of any kind, and both had displayed different properties and performance results, particularly in terms of mechanical properties.

These findings showed that bioplastic films formed in this research has weak mechanical properties. The values mentioned earlier indicated that the film has a low tensile strength does not meet the standard values of moderate grade of bioplastic, which ranges from 1 to 10 N/mm^2 of tensile strength [42]. Hence, the bioplastic films produced in this study may not be suitable for applications that require high strength and durability.

Moving forward, for applications demanding higher mechanical strength, it is beneficial to explore formulation adjustments that will improve the tensile properties of the bioplastic films. This could involve optimizing the cellulose distribution within the matrix or incorporating reinforcing agents such as microcrystalline cellulose [28].

3.6. Thermogravimetric analysis (TGA)

The TGA curves for BF-0.30, BF-0.50, and BF-0.70 in Fig. 6 show that there were slight weight losses of about 10% that occurred between 30 °C and 200 °C. These weight losses were caused by the moisture content evaporating [43] and the breakdown of weaker bonds in the structure of the bioplastic films [44].

The TGA analysis showed that BF-0.10, BF-0.30, BF-0.50, and BF-0.70 had rapid and significant composition in approximately 200 °C and 400 °C range. This can be attributed to the decomposition of cellulose in the bioplastic films [29]. At this stage, BF-0.10 was the bioplastic film with the lowest initial decomposition temperature, at about 30 °C. Conversely, at 193 °C, BF-0.70 had the highest initial decomposition temperature. This was probably due to the higher content of

cellulose in BF-0.70, as well as the good morphological properties possessed by BF-0.70 as compared to the other bioplastic films as discussed in Section 3.5.
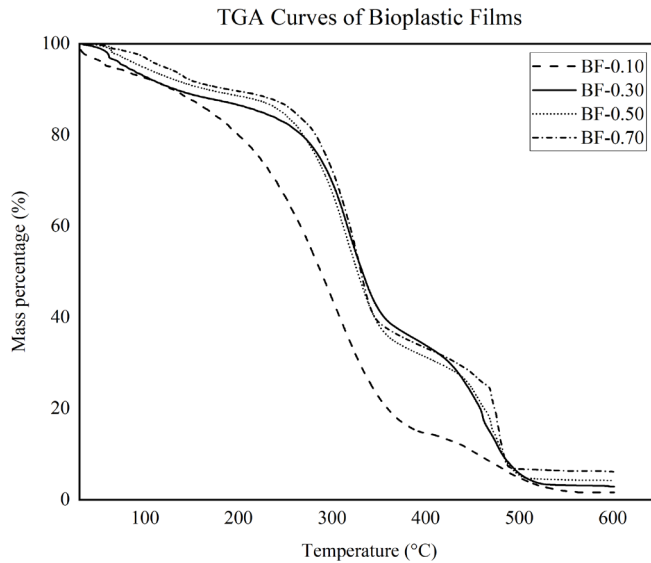

Fig. 6. TGA curve of bioplastic films.

The weight losses of approximately 12% to 27% corresponded to non-cellulosic component, around 380 °C to 500 °C for the TGA analysis, was found to be lignin based on previous research, which can be observed in all four bioplastic films [45]. This supports the notion that lignin was probably present as a component in the bioplastic as discussed in Section 3.1.

Figure 7 showed the estimated percentage of char residue of BF-0.10, BF-0.30, BF-0.50, and BF-0.70 after 600 °C. It was observed that the residue increased as the amount of CF increased, hence the increase in amount of non-cellulosic components such as lignin. The aromatic structures in lignin were thermally more stable and mostly remained in the char residue formed during heating [46]. In addition, the thermal stability of the bioplastic film can also be determined by measuring the amount of char residue that is left over after heating. A larger mass of char residue, which is showed by BF-0.70, suggests that the bioplastic film is less prone to degradation and more thermally stable [47].

In comparison, the char residue formed for bioplastic films from sago starch with cellulose fibres from SPW [14] was around 0.73%, which was lower than this research's bioplastic film char residue, which was around 6.12% for BF-0.70. The lower char residue of the sago starch with cellulose fibre bioplastic film was probably due to the lower degradation temperature of starch [38].

All in all, BF-0.10 had the lowest initial decomposition temperature of cellulose, which was the main part of the bioplastic film and the lowest char residue among all the other bioplastic films, which indicated that BF-0.10 was the least thermally stable. In contrary, the BF-0.70 had the highest initial decomposition temperature and the highest amount of char residue. This concluded that BF-0.70 was the most thermally stable.
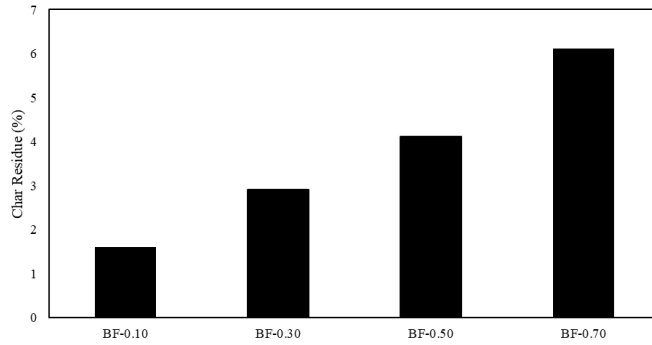
Fig. 7. Char residue of bioplastic films after 600 °C.

3.7. Water absorption

Table 6 and Fig. 8 showed the water absorption of all four bioplastic films, BF-0.10, BF-0.30, BF-0.50, and BF-0.70. All four of the bioplastic films that had undergone the analysis demonstrated unfavourable water absorption characteristics, showing a notable tendency for high water absorption. This is probably due to the natural hydrophilic properties of cellulose. Cellulose has hydroxyl groups (OH) which allows it to form hydrogen bonds with water molecules, leading to their strong affinity for water [39].
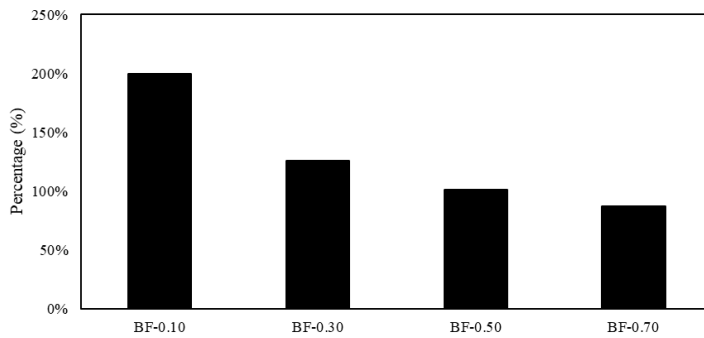

Fig. 8. Water absorption of bioplastic films.

The increment of pores presence as the mass of CF increased in bioplastic films had also influenced the water absorption of the bioplastic film. The SEM images that had been shown in Fig. 4 proved that all bioplastic films in this research had noticeable pores and it became less obvious as the mass of CF to form bioplastic films increased. This had been contributing to the number of pathways for the water molecules to enter the bioplastic film which led to a faster water absorption process [48].

As a comparison, for sago starch with cellulose fibres bioplastic film formed by Yacob and his team, the amount water absorption decreased as the number of cellulose fibres in the starch matrix increased. This was due to the restriction of the matrix chain mobility, which had resulted in lower ability of the water molecules to enter the bioplastic films [49]. Their lowest percentage for the amount of water absorption was 120%. Although BF-0.70 had lower amount of water absorption between the two bioplastic films, the amount of water absorption both bioplastic

films were quite high as starch and cellulose are both hydrophilic materials, meaning they had a strong affinity for water molecules.

The practical application of bioplastic films is greatly influenced by their rate of water absorption. For example, bioplastic films may lose some of their mechanical strength as a result of high-water absorption [50]. This could lead to decreased structural integrity, which would make them less appropriate for some uses that require resistance to moisture. Bioplastics' low moisture resistance also hinders their growth and use in wider application; therefore, more research is needed to find reinforcing agents that can give these bioplastic films hydrophobic qualities, which will increase their moisture resistance [51].

Table 6. Water absorption results.

	Sample 1 (%)	Sample 2 (%)	Sample 3 (%)	Mean (%)	Standard deviation (%)
BF-0.10	195	202	198	198	3.51
BF-0.30	130	123	125	126	3.61
BF-0.50	105	101	102	103	2.08
BF-0.70	90	85	84	86	3.21

3.8. Limitations and challenges

Although our study provides insightful information about bioplastic films, it is crucial to acknowledge certain limitations and difficulties. First, there is the sensitivity of measurement techniques. Tensile strength and Young's modulus are measured using methods that are sensitive to humidity and temperature. Even with the best efforts, minor fluctuations could have affected the precision of the resulting measurements due to these factors.

To address the challenge of very low tensile strength in our bioplastic films, the addition of reinforcing agents should be explored more in the future. Upcoming research could be carried out to identify a suitable combination of reinforcing agents. The mechanical properties of the bioplastic films can be improved by reinforcing agents such as microcrystalline cellulose during the solubilisation of CF in the TFA [28]. By adding these additives, the mechanical properties and thermal stability of the bioplastic films may be altered.

For future reference, the solubilisation time of the CF in TFA solution can also be improved by adding trifluoroacetic anhydride (TFAA) to the mixture of TFA before the solvent casting process. Shorter solubilisation period can reduce energy consumption and improve process efficiency [17].

It was also acknowledged that long-term performance and biodegradation aspects were not widely explored. Future research could explore deeper into these aspects, contributing to a more thorough evaluation of the material's sustainability.

4. Conclusions

The extraction of cellulose from SPW was successfully done through alkaline and bleaching treatment. Observationally, bleached cellulose fibres extracted from SPW changed colour to white, which exhibited that most of the original non-cellulosic components had been removed. Free-standing bioplastic films were

successfully formed by using the resulting CF. One standout discovery was the identification of the optimal CF mass, a critical parameter for forming bioplastic films. The findings found that solubilising 0.70 g of CF per 20 mL of TFA leads to a great improvement in morphological properties, tensile strength, and thermal stability, as demonstrated by the characteristics of BF-0.70.

Overall, observation of BF-0.70 demonstrated a significant reduction in bubble-shape protrusions, and the number of visible pores decreased significantly compared to lower CF masses. The significant improvement in tensile strength that results from this improved morphology is noteworthy, as demonstrated by the notable 90% increase in tensile strength of BF-0.70 when compared to BF-0.10. The reduction in structural irregularities and increased tensile strength can be ascribed to the higher cellulose content, which helps better intermolecular bonding within and between cellulose chains in the bioplastic films.

Furthermore, the improvement in morphological properties correlates with the observed reduction in water absorption for BF-0.70, which showed a significant 150% decrease compared to bioplastic films with lower CF masses. The optimal CF mass of 0.70 g per 20 mL of trifluoroacetic acid (TFA) not only exhibited improved morphological properties, increased tensile strength, and a reduction in water absorption, but also demonstrated good thermal stability, as it was observed that the char residue has tripled the amount of the char residue of BF-0.10.

All in all, this study is the first to use SPW for making bioplastic films by using TFA. By extracting cellulose and forming bioplastic films with TFA, a new way was discovered to repurpose SPW. This approach adds something new to existing research on cellulose-based bioplastics. It is a practical step towards sustainability and broadens the possibilities in bioplastic research.

Nomenclatures	
w_0	Initial weight of sample
w_1	Final weight of sample
Abbreviations	
BF	Bioplastic film
CF	Cellulose fibres
FTIR	Fourier transform infrared
FTIR-ATR	Fourier transform infrared attenuated total reflectance
SEM	Scanning electron microscope
SPW	Sago pith waste
SSCMF	Sago starch filled with cellulose microfibres
TFA	Trifluoroacetic acid
TGA	Thermogravimetric analysis
TS	Tensile strength

References

1. Marrone, B. (2022). Bioplastics point the way to an environmentally sustainable, green future. Retrieved July 8, 2023, from https://discover.lanl.gov/news/0426-bioplastics/.

2. Ali, W.; Ali, H.; Souissi, S.; and Zinck, P. (2023). Are bioplastics an ecofriendly alternative to fossil fuel plastics?. *Environmental Chemistry Letters*, 21(4), 1991-2002.

3. Filho, W.L. et al. (2022). Consumer attitudes and concerns with bioplastics use: An international study. *PLoS ONE*, 17(4), 1-16.

4. Lamberti, F.M.; Román-Ramírez, L.A.; and Wood, J. (2020). Recycling of bioplastics: routes and benefits. *Journal of Polymers and the Environment*, 28(10), 2551–2571.

5. Gomes, M.P.; Pereira, E.G.; Qiu, B.S.; and Juneau, P. (2021). Coping with pollution – the effects of environmental contaminants on plant growth and physiology. *Frontiers in Plant Scienc*e, 12(1), 1807.

6. Lim, L.W.K.; Chung, H.H.; Hussain, H.; and Bujang, K. (2019). Sago palm (Metroxylon sagu Rottb.): Now and beyond. *Pertanika Journal of Tropical Agricultural Science*, 42(2), 435-451.

7. Zhu, F. (2019). Recent advances in modifications and applications of sago starch. *Food Hydrocolloids*, 96, 412-423.

8. Wong, J. (2022). Sarawak pushing for sago cultivation. Retrieved November 16, 2022, from https://www.thestar.com.my/business/business-news/2022/02/21/sarawak-pushing-for-sago-cultivation.

9. Susanti, T.L.; Safitri, R.; and Padmadijaya, A.H. (2022). Utilization of sago dregs as ruminant feed by using the fermentation method: Literature review. *Jurnal Bioteknologi and Biosains Indonesia*, 9(2), 268-282.

10. Mering, M.N.; Bolhassan, M.H.; and Awg-Adeni, D.S. (2022). The physical characteristics and yield of grey oyster mushroom (Pleurotus sajor-caju) cultivated on sawdust and sago hampas as substrate. *Asia-Pacific Journal of Molecular Biology and Biotechnology*, 30(2), 44-53.

11. Rasyid, T.H.; Kusumawaty, Y.; and Hadi, S. (2020). The utilization of sago waste: Prospect and challenges. *Proceedings of the IOP Conference Series: Earth and Environmental Science*, *INAFOR EXPO* 2019 - *International Conference on Forest Products (ICFP)*, Bogor, West Java, Indonesia, 415(1), 012023.

12. Adejumo, I., and Adebiyi, O. (2020). Agricultural solid wastes: Causes, effects, and effective management. In H.M. Saleh (Ed.). *Strategies of sustainable solid waste management*. IntechOpen.

13. Tan, S.X. et al. (2021). Rapid ultrasound-assisted starch extraction from sago pith waste (SPW) for the fabrication of sustainable bioplastic film. *Polymers*, 13(24), 4398.

14. Yacob, N.; Yusof, M.R.; Ainun, Z.M.A.; and Badri, K.H. (2018). Effect of cellulose fiber from sago waste on properties of starch-based films. *Proceedings of the IOP Conference Series: Materials Science and Engineering*, 368(1), 012028.

15. Jampi, A.L.W.; Chin, S.F.; Wasli, M.E.; and Chia, C.H. (2021). Preparation of cellulose hydrogel from sago pith waste as a medium for seed germination. *Journal of Physical Science*, 32(1), 13-26.

16. Bilo, F. et al. (2018). A sustainable bioplastic obtained from rice straw. *Journal of Cleaner Production*, 200, 357-368.

17. Tedeschi, G. et al. (2020). Multifunctional bioplastics inspired by wood composition: Effect of hydrolyzed lignin addition to xylan-cellulose matrices. *Biomacromolecules*, 21(2), 910-920.

18. Zhang, X.; Qu, T.; Mosier, N.S.; Han, L.; and Xiao, W. (2018). Cellulose modification by recyclable swelling solvents. *Biotechnology for Biofuels*, 11, 1-12.

19. Farid, M. at al. (2021). *Production of bioplastics by different methods-a step toward green economy: A review*. Tahir, M.B.; Rafique, M.; and Sagir, M. (Eds.), Nanotechnology, Springer, Singapore.

20. Liang, K.; Zhu, H.; and Zhang, Y. (2022). Effect of mechanical grinding on the physicochemical, structural, and functional properties of foxtail millet (Setaria italica (L.) P. Beauv) bran powder. *Foods*, 11(17), 2688.

21. Arnata, I.W.; Suprihatin, S.; Fahma, F.; Richana, N.; and Sunarti, T.C. (2019). Cellulose production from Sago frond with alkaline delignification and bleaching on various types of bleach agents. *Oriental Journal of Chemistry*, 35(Special Issue 1), 8-19.

22. Al kamzari, S.M.A. et al. (2023). Extraction and characterization of cellulose from agricultural waste materials. *Materials Today: Proceedings*, 80(3), 2740-2743.

23. Pushpamalar, V.; Langford, S.J.; Ahmad, M.; and Lim, Y.Y. (2006). Optimization of reaction conditions for preparing carboxymethyl cellulose from sago waste. *Carbohydrate Polymers*, 64(2), 312-318.

24. Wang, T.; and Zhao, Y. (2021). Optimization of bleaching process for cellulose extraction from apple and kale pomace and evaluation of their potentials as film forming materials. *Carbohydrate Polymers*, 253, 117225.

25. Raju, V. et al. (2023). Isolation and characterization of nanocellulose from selected hardwoods, viz., Eucalyptus tereticornis Sm. and Casuarina equisetifolia L., by steam explosion method. *Scientific Reports*, 13(1), 1-15.

26. Bayer, I.S. et al. (2014). Direct transformation of edible vegetable waste into bioplastics. *Macromolecules*, 47(15), 5135-5143.

27. Bayer, I.S.; Mele, E.; Fragouli, D.; Cingolani, R.; and Athanasiou, A. (2019). Process for the production of biodegradable plastics material from cellulose plant wastes. *Patent EP3063176A1*. European Patent Office.

28. Guzman-Puyol, S. et al. (2017). Facile production of seaweed-based biomaterials with antioxidant and anti-inflammatory activities. *Algal Research*, 27, 1-11.

29. Guzman-Puyol, S. et al. (2022). Transparent, UV-blocking, and high barrier cellulose-based bioplastics with naringin as active food packaging materials. International *Journal of Biological Macromolecules*, 209, 1985-1994.

30. Fareez, I.M. et al. (2018). Characteristics of cellulose extracted from Josapine pineapple leaf fibre after alkali treatment followed by extensive bleaching. *Cellulose*, 25, 4407-4421.

31. Sirviö, J.A. (2019). Fabrication of regenerated cellulose nanoparticles by mechanical disintegration of cellulose after dissolution and regeneration from a deep eutectic solvent. *Journal of Materials Chemistry A*, 7(2), 755-763.

32. Hospodarova, V.; Singovszka, E.; and Stevulova, N. (2018). Characterization of cellulosic fibers by FTIR spectroscopy for their further implementation to building materials. *American Journal of Analytical Chemistry*, 9, 303-310.

33. Zhang, T., Zhang, Y., Jiang, H. and Wang, X. (2019). Aminosilane-grafted spherical cellulose nanocrystal aerogel with high CO2 adsorption capacity. *Environmental Science and Pollution Research*, 26(16), 16716-16726.

34. Monika (2018). Bonding of trifluoroacetic acid with cellulose. *IOSR Journal of Applied Chemistry (IOSR-JAC)*, 11(2), 71-74.

35. Tabaght, F.E. et al. (2023). Synthesis, characterization, and biodegradation studies of new cellulose-based polymers. *Scientific Reports*, 13(1), 1-15.

36. Nigam, S.; Das, A.K.; and Patidar, M.K. (2021). Valorization of Parthenium hysterophorus weed for cellulose extraction and its application for bioplastic preparation. *Journal of Environmental Chemical Engineering*, 9(4), 105424.

37. Gurram, R.; Souza Filho, P.; Taherzadeh, M.; and Zamani, A. (2018). A solvent-free approach for production of films from pectin and fungal biomass. *Journal of Polymers and the Environment*, 26, 4282-4292.

38. Syafri, E. et al. (2019). Characterization and properties of cellulose microfibers from water hyacinth filled sago starch bio-composites. *International Journal of Biological Macromolecules*, 137, 119-125.

39. Wohlert, M. et al. (2022). Cellulose and the role of hydrogen bonds: Not in charge of everything. *Cellulose*, 29, 1-23.

40. Nguyen, T.K.; That, N.T.T.; Nguyen, N.T.; and Nguyen, H.T. (2022). Development of starch-based bioplastic from jackfruit seed. *Advances in Polymer Technology*, 2022, 6547461.

41. Zamrud, Z., Ng, W.M. and Salleh, H.M. (2021). Effect of bentonite nanoclay filler on the properties of bioplastic based on sago starch. *Proceedings of the IOP Conference Series: Earth and Environmental Science*, 765(1), 12009.

42. Nasir, N.N.; and Othman, S.A. (2021). The physical and mechanical properties of corn-based bioplastic films with different starch and glycerol content. *Journal of Physical Science*, 32(3), 89-101.

43. Steven, S.; Fauza, A.N.; Mardiyati, Y.; Santosa, S.P.; and Shoimah, S.M. (2022). Facile preparation of cellulose bioplastic from Cladophora sp. algae via hydrogel method. *Polymers*, 14(21), 4699.

44. Obande, W. et al. (2021). Enhancing the solvent resistance and thermomechanical properties of thermoplastic acrylic polymers and composites via reactive hybridisation. *Materials & Design*, 206, 109804.

45. Trilokesh, C.; and Uppuluri, K.B. (2019). Isolation and characterization of cellulose nanocrystals from jackfruit peel. *Scientific Reports*, 9(1), 1-8.

46. Liang, J. et al. (2023). Interaction of derivatives of cellulose and lignin in co-HTC, co-pyrolysis and co-activation. *Fuel*, 351, 129033.

47. Charles, A.L.; Motsa, N.; and Abdillah, A.A. (2022). A comprehensive characterization of biodegradable edible films based on potato peel starch plasticized with glycerol. *Polymers*, 14(17), 3462.

48. Oluwasina, O.O.; Olaleye, F.K.; Olusegun, S.J.; Oluwasina, O.O.; and Mohallem, N.D.S. (2019). Influence of oxidized starch on physicomechanical,

thermal properties, and atomic force micrographs of cassava starch bioplastic film. *International Journal of Biological Macromolecules*, 135, 282-293.

49. Yacob, N.; Yusof, M.R.; Mohamed, A.Z.; and Badri, K.H. (2019). Effect of cellulose fiber loading on the properties of starch-based films. *Proceedings of the Universiti Kebangsaan Malaysia, Faculty of Science and Technology 2018 Postgraduate Colloquium*, Selangor, Malaysia, 2111(1), 050009.

50. Judawisastra, H.; Sitohang, R.D.R.; Marta, L.; and Mardiyati (2017). Water absorption and its effect on the tensile properties of tapioca starch/polyvinyl alcohol bioplastics. *Proceedings of the IOP Conference Series: Materials Science and Engineering*, Medan, Indonesia, 223(1), 012066.

51. Shafqat, A.; Al-Zaqri, N.; Tahir, A.; and Alsalme, A. (2021). Synthesis and characterization of starch based bioplatics using varying plant-based ingredients, plasticizers and natural fillers. *Saudi Journal of Biological Sciences*, 28(3), 1739-1749.